Journal of Physics: Condensed Matter

PAPER

Activation energy, spatial confinement, and mean first passage and escape times of a tracer in a wormlike micellar fluid: an effective potential approach

To cite this article: Guillermo Iván Guerrero-García *et al* 2022 *J. Phys.: Condens. Matter* **34** 174006

View the article online for updates and enhancements.

You may also like

- Structural characterization of Di-C_{12} P-uridine worm-like micelles: ionic strength dependence
F Baldelli Bombelli, F Betti, D Berti et al.
- Transient dynamics of a colloidal particle driven through a viscoelastic fluid
Juan Ruben Gomez-Solano and Clemens Bechinger
- Group theory and biomolecular conformation: I. Mathematical and computational models
Gregory S Chirikjian

This content was downloaded from IP address 129.105.215.146 on 15/08/2023 at 16:07

IOP Publishing Journal of Physics: Condensed Matter
J. Phys.: Condens. Matter **34** (2022) 174006 (10pp) https://doi.org/10.1088/1361-648X/ac4fe6

Activation energy, spatial confinement, and mean first passage and escape times of a tracer in a wormlike micellar fluid: an effective potential approach

Guillermo Iván Guerrero-García[1,*], **Daniela Pérez-Guerrero**[2] **and Erick Sarmiento Gómez**[3]

[1] Facultad de Ciencias de la Universidad Autónoma de San Luis Potosí, Av. Chapultepec 1570, Privadas del Pedregal, 78295, San Luis Potosí, México
[2] Instituto de Física de la Universidad Autónoma de San Luis Potosí, Álvaro Obregón 64, 78000 San Luis Potosí, San Luis Potosí, México
[3] División de Ciencias e Ingenierías, Universidad de Guanajuato, Loma del Bosque 103, 37150 León,México

E-mail: givan@uaslp.mx

Received 1 November 2021, revised 13 January 2022
Accepted for publication 28 January 2022
Published 25 February 2022

Abstract

Wormlike micelles are long semiflexible cylindrical polymer structures formed by amphiphiles. In solution, these linear micelles percolate in multiconected entangled networks, where cross-links can break and recombine dynamically. Technological applications of wormlike micellar fluids include tunable encapsulation/delivery of molecules or colloids in biomedicine, oil industry, and/or cleaning processes. In this work, we propose that the experimental activation energy, the spatial confinement, and the mean first passage and escape times of a spherical tracer immersed in wormlike micellar network, in which caging effects are observed, can be estimated from economic Brownian dynamics simulations of a single particle interacting with an effective one-dimensional cosine-like potential of amplitude U_0 and periodicity L. The proposed one-fitting parameter method has been used to characterize the long-time dynamics of wormlike micellar solutions formed by the self-assembly of a mixture of zwitterionic and anionic surfactants at several temperatures and different concentrations of surfactant and brine. The amplitude U_0 has displayed a good agreement regarding the corresponding experimental activation energy at different temperatures. The periodicity L has shown to be an upper bound of the mesh size ξ and of the same order of magnitude regarding the entanglement length l_e, obtained from rheology and microrheology experiments. The escape time of the tracer in the effective potential τ_{escape} and the time t^*, at which a change of curvature in the mean square displacement occurs, are upper and lower limits, respectively, of the experimental relaxation time. Our method is simple and fast, and we foresee that it should be applicable to model the long-time behaviour of tracers in other polymer systems, in which caging effects are present.

Keywords: first passage time, wormlike micelles, polymers, effective potential, long-times diffusion, caging effects, Bellour parametrization

(Some figures may appear in colour only in the online journal)

* Author to whom any correspondence should be addressed.

 © 2022 IOP Publishing Ltd Printed in the UK

1. Introduction

Amphiphilic molecules are found to self-assemble in aqueous solutions and form complex structures in several geometries, ranging from simple spherical micelles and elongated structures such as wormlike micelles, to quasi 2D structures such as lamellar, sponge and other topologically complex phases, just to mention a few [1, 2]. Each structure has unique and particular properties that can be used in technological applications [3]. In particular wormlike micelles, due to the presence of elongated structures, are capable of store mechanical energy during a deformation, thus presenting a viscoelastic response to the solution where they are embedded [4]. As the time scale of the deformation is directly related with the typical excited structure, the response varies from a viscous to an elastic behaviour at different times essentially. For example, for an step-strain experiment, the response changes from an elastic to a viscous material. The so called relaxation time, which indicates the crossover between regimes, is also highly dependent on the physical and chemical properties of the system. Depending on the studied system, different mechanisms are related to the elastic properties. In a typical polymeric system, the polymer itself is able to store energy by deformation [5]. In addition, a relaxation process is observed due to the diffusion of the polymer, which releases stress and produces a relaxation spectra with multiple characteristic times. Cates and co-workers found that a breaking polymer, with a breaking time shorter than the typical diffusion time, behaves with a unique relaxation time [6]. Soon after this, it was found that the self-assembly of surfactants in elongated structures can be approximated by an unique relaxation time [7]. In this case, the polymer-like breaking is an activated and temperature-dependent process displaying an Arrhenius behavior typically. Such comportment is quite different to the classical behaviour displayed by a polymer, in which the dependence on time is only related to a diffusion mechanism [5]. Thus, the activation energy is also a very important parameter that characterises the polymer relaxation. Other parameters have been found to be useful to characterise the structure of a polymer-like network such as the mesh size, which allows us to know approximately the free available space among polymers. In this regard, it has also been observed that this size is related directly to the elastic modulus [5]. Thus, the development of experimental and theoretical tools for predicting the activation energy, relaxation time and characteristic lengths of a polymer-like system is still of paramount importance for the physico-chemical community with some examples of such methods already found in the literature [8–13]. These tools are also helpful to characterize the experimental systems and can be useful to predict the physical properties required for specific applications.

In general, important parameters of the mechanical resp onse of a polymer-like system can be obtained by performing numerical simulations [14]. In such a scenario, the equations of motion are numerically evaluated and solved in a computer in order to obtain the corresponding structure as a function of time. However, a suitable model for the intermolecular interactions is needed, and, depending on the required computational time and system size, numerical simulations of polymer-like systems over several decades of time can be very expensive computationally. Moreover, extracting the mechanical response properties often requires complex methodologies. From an experimental point of view, it is possible to perform direct measurements of the macroscopic mechanical properties using devices such as a rheometer. In this case, the torque exerted on a mechanical geometry can be related to the stress response under a particular deformation [18]. However a theoretical framework is still required to relate the mechanical properties to either the activation energy or the characteristic lengths of the system. Moreover, this often requires information that cannot be extracted from a typical rheometer [8–13]. On the other hand, other experimental methods can be used to obtain the physical properties of the polymer-like structure by direct measurement of the motion of molecules, such as NMR and neutron scattering experiments, for example [13, 15–17]. An alternative indirect method is to track the motion of a micrometer tracer particle on the polymer-like structure in order to extract the structural relaxation from the dynamics displayed by the tracer particle. This technique is called microrheology, and it is based on a generalized Langevin equation that includes information related to the microscopic friction and the macroscopic viscosity [9–11, 19]. Thus, observing the Brownian motion of a tracer particle allows us to extract viscoelastic properties of a polymer-like network in a wider range of times regarding a typical rheological apparatus. Using, for example, light scattering techniques, the Brownian motion can be extracted in several decades of time, providing then information of the viscoelastic spectra in a wider range [20]. This opens the possibility of using this kind of results to extract several characteristic lengths of a polymer-like system. As we will see below, the contribution of this work relies on a new and more efficient methodology to extract some characteristic properties of such networks by using an effective potential approach.

On the other hand, Lifson and Jackson [21] proposed in the 60s to use a one-dimensional periodic potential to determine the dynamic properties of colloidal particles immersed in a supporting polyelectrolyte solution. In particular, they found

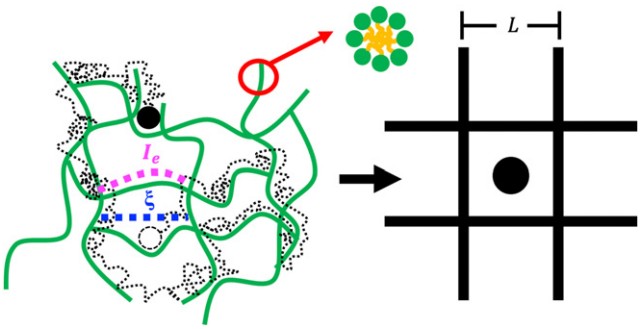

Figure 1. 2D representation of a tracer immersed in a WM solution and the corresponding effective model. ξ is the mesh size and l_e is the entanglement length.

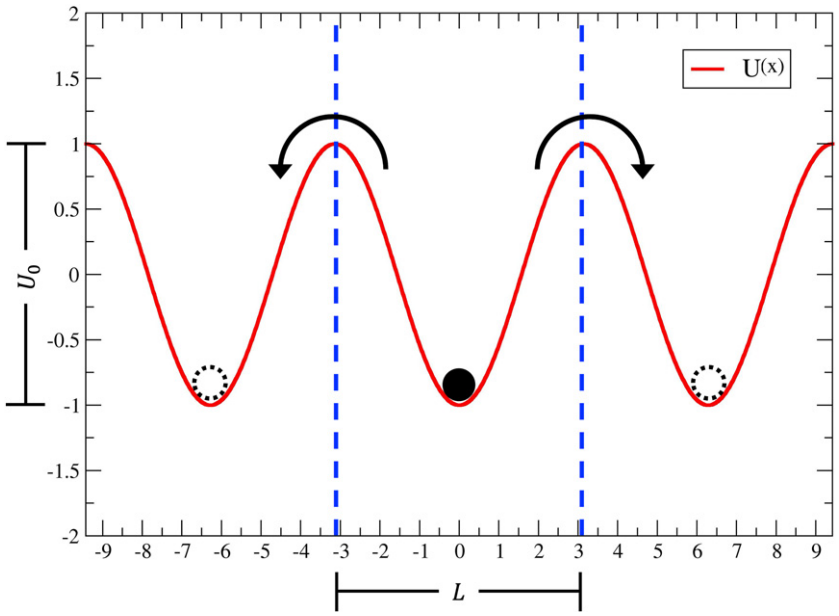

Figure 2. Cosine potential. The separatrix manifold is represented as a vertical blue dashed line.

that the ratio of the long- and short-time diffusion coefficient of a colloidal particle could be calculated as the expected value of a function that depended on an effective periodic potential, with a spatial periodicity L and maximum height U_0. This mathematical result has been demonstrated by other authors using different approaches [22, 23]. In this work, we propose to use a simple periodic cosine potential as an effective periodic potential to estimate the activation energy of a spherical tracer in a wormlike micellar (WM) polymer network, if the experimental parametrization of the mean square displacement (MSD) of the tracer in terms of the phenomenological Bellour equation is known. Afterwards, we propose to adjust the width L of the periodic effective potential in a Brownian dynamics simulation to reproduce the experimental MSD at the time t^*, at which a change of curvature occurs. If we follow this prescription, our numerical Brownian dynamics results display that (i) the periodicity L of the effective potential is an upper bound of the experimental mesh size ξ and is of the same order of magnitude regarding the entanglement length l_e, and (ii) it is possible to estimate of the escape and the mean first passage time (MFPT) of a particle under the influence of the effective periodic potential of amplitude U_0 and periodicity L, providing upper and lower bounds for the relaxation time of the viscoelastic material.

2. Model and methods

A two-dimensional representation of a tracer immersed in a WM solution and the corresponding effective model are depicted in figure 1, where the complexity of a random localization of the wormlike micelles giving the interconnected network, and hindering the motion of the tracer, is reduced using a simpler periodic structure with a characteristic length L.

The effective one dimensional potential we propose is a simple cosine potential of the form:

$$U(x, U_0, L) = U_0 \left(1 - \cos\left(\frac{2\pi x}{L}\right)\right), \tag{1}$$

where U_0 and L are the amplitude and periodicity of the external potential, respectively, as shown in figure 2. Overdamped Brownian dynamics simulations are performed using the method proposed by Ermak and McCammon without hydrodynamic interactions [24]. According to this prescription, the position of the particle at time $t + \mathrm{d}t$ is calculated from the previous position at time t by using the equation:

$$x(t + \mathrm{d}t) = x(t) + \frac{D_0 F(x(t))\mathrm{d}t}{k_B T} + R(\mathrm{d}t), \tag{2}$$

where D_0 is the translational diffusion coefficient of the particle at short-times, $F(x) = -\frac{\mathrm{d}U(x)}{\mathrm{d}x}$ is the force that the particle experiences due to the external periodic potential $U(x)$, and $R(\mathrm{d}t)$ is a random displacement, having a normal distribution with zero mean value and variance $2D_0\,\mathrm{d}t$, fulfilling the so-called fluctuation–dissipation theorem. In Brownian dynamics simulations, the magnitude of the time step $\mathrm{d}t$ is crucial. If it is too short, the computational time can increase significantly. If it is too large, the stochastic differential equation can display incorrect values of the dynamic properties of the system. A time step of 3 μs allowed us to reproduce the analytic MSD of the Brownian harmonic oscillator with an error lower than 1 percent for a wide range of spring constants. In a typical Brownian dynamics simulation a maximum $N_{\max} = 1 \times 10^{11}$ times steps have been performed, which is equivalent to a total time of 3×10^5 s. Once the positions of the tracer are known as a function of time and assuming that the statistical

Table 1. Experimental activation energies E_a^{Exp} of a spherical tracer of 800 nm of diameter immersed in WM solutions with zwitterionic surfactant TDPS, anionic surfactant SDS and brine reported in reference [34] at several temperatures and different concentrations of brine, keeping constant the zwitterionic surfactant concentration $C_z = 46$ mM. The brine concentration [NaCl] is 0.5 M and 0.225 M for $R = 0.45$ and $R = 0.55$, respectively, where $R = [SDS]/[TDPS]$ is the surfactant ratio. U_0 is the one-dimensional height barrier obtained in this work from equation (6), by using D_0^{Exp} and D_M^{Exp} from reference [11] The uncertainty of U_0 is less than 1 percent.

T (C)	R	E_a^{Exp} (KJ mol^{-1})	D_0^{Exp} (m^2 s^{-1})	D_M^{Exp} (m^2 s^{-1})	$U_0[k_BT]^{This\ work}$	$3U_0$ (KJ mol^{-1})$^{This\ work}$
20	0.45	53 ± 7	4.20×10^{-13}	9.72×10^{-18}	7.23	52.79
25	0.45	53 ± 7	3.86×10^{-13}	1.57×10^{-17}	6.92	51.43
30	0.45	53 ± 7	3.16×10^{-13}	2.26×10^{-17}	6.62	49.98
20	0.55	62 ± 1	3.95×10^{-13}	7.53×10^{-19}	8.56	62.55
25	0.55	62 ± 1	5.20×10^{-13}	1.45×10^{-18}	8.36	62.12
30	0.55	62 ± 1	3.56×10^{-13}	3.21×10^{-18}	7.73	58.41

properties do not depend on the initial time, the MSD can be calculated as:

$$\mathrm{MSD}(t_j) = \frac{1}{N_{\max} - j} \sum_{i=1}^{N_{\max}-j} [x(t_i + j\,\mathrm{d}t) - x(t_i)]^2, \qquad (3)$$

where $t_i = i\,\mathrm{d}t$.

In spite of the simplicity of the periodic potential defined by equation (1), interesting phenomena have been reported in the literature when this potential has been applied to colloidal systems as an external field: from the experimental point of view, it is found that a colloidal particle subjected to such potential presents a diffusive regime at short times with a diffusion coefficient corresponding to free diffusion, followed by a caging dynamics due to the trapping effect of the potential, and finally a second linear regime is found, with a diffusion coefficient that can be orders of magnitude lower that the first regime [28]; it has been seen a freezing-melting transition due to the interaction between particles trapped in neighbouring minima [25]; numerical simulations have shown that the competition between both particle–particle and particle–substrate interactions leads to a rich variety of adsorbate phases or particle distributions [26]; optical ray tracing calculations have shown interesting energy landscapes in the presence of anisotropic colloidal particles [27]; the long- and short-times diffusion coefficient ratio has been studied comprehensively as a function of the height barrier U_0 in equation (1) via experiments and numerical calculations in the absence of hydrodynamic interactions [28], and numerically in the presence of hydrodynamic interactions [29]; the long-times dynamics of a colloidal tracer under the influence of an external potential given by equation (1) has been studied via numerical simulations, at non-low height barrier U_0 values, showing that (i) the most likely first passage time of the tracer is roughly independent of the height barrier U_0, and (ii) the most likely first passage time of the tracer can be approximated, as a first approximation, as the specific time at which occurs a change of curvature in the corresponding MSD [30].

According to Bellour *et al* [31], the dynamics of a spherical tracer immersed in a WM solution follows roughly the same dynamical regimes as the previously explained for the sinusoidal potential and can be accurately fitted to the following four-parameters phenomenological equation:

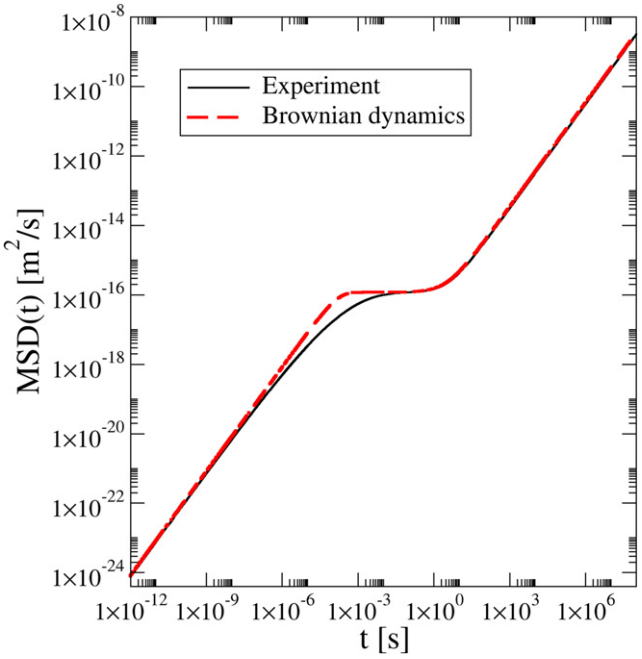

Figure 3. Mean square displacement MSD(t) of a spherical tracer immersed in a WM solution at a temperature $T = 25$ C and $R = 0.45$, with the following Bellour parameters obtained from experimental data reported in reference [11]: $D_0^{Exp} = 3.86 \times 10^{-13}$ m^2 s^{-1}, $D_M^{Exp} = 1.57 \times 10^{-17}$ m^2 s^{-1}, $2\delta^{Exp} = 1.17 \times 10^{-16}$ m^2, and $\alpha^{Exp} = 0.274$. Brownian dynamics used a short-times diffusion coefficient $D_0 = D_0^{Exp}$, and an amplitude $U_0 = 6.92/(k_BT)$ and periodicity $L = 1.20 \times 10^{-7}$ m in the effective one-dimensional potential.

$$\mathrm{MSD}^{\mathrm{Bellour}}(t, D_0, D_M, \alpha, \delta) = 2\delta^2 \left(1 - \exp\left\{-\left(\frac{D_0 t}{\delta^2}\right)^{\alpha}\right\}\right)^{\frac{1}{\alpha}} \left(1 + \frac{D_M t}{\delta^2}\right), \qquad (4)$$

where D_0 and D_M are the short- and long-time diffusion coefficients of the tracer corresponding to the free diffusion at short times and the hopping process at the macro scale. α and δ are fitting parameters that allow us to reproduce the onset of the plateau displayed by the experimental MSD, which is more conspicuous at large activation energies. The Bellour model contains partially the solution to the Langevin equation

Table 2. Bellour parameters D_0^{Exp}, $D_{\mathrm{M}}^{\mathrm{Exp}}$, δ^{Exp}, and α^{Exp} associated to experimental MSD curves of a spherical tracer of 800 nm of diameter immersed in WM solutions with zwitterionic surfactant TDPS, anionic surfactant SDS and brine reported in reference [11] at several temperatures and different concentrations of brine, keeping constant the zwitterionic surfactant concentration $C_z = 46$ mM. The brine concentration [NaCl] is 0.5 M and 0.225 M for $R = 0.45$ and $R = 0.55$, respectively, where $R =$ [SDS]/[TDPS] is the surfactant ratio. U_0 was obtained in this work from equation (6). By using $D_0 = D_0^{\mathrm{Exp}}$ and U_0 as fixed parameters in Brownian dynamics simulations, the width L of the periodic effective potential was adjusted until the simulation and the experimental MSD were approximately the same at the critical time t^*, where a change of curvature in the MSD is observed.

T (C)	R	D_0^{Exp} (m^2 s^{-1})	$D_{\mathrm{M}}^{\mathrm{Exp}}$ (m^2 s^{-1})	$2\delta^{2\mathrm{Exp}}$ (m^2)	α^{Exp}	$U_0[k_{\mathrm{B}}T]^{\mathrm{This\ work}}$	L (m)$^{\mathrm{This\ work}}$
20	0.45	4.20×10^{-13}	9.72×10^{-18}	1.12×10^{-16}	0.310	7.23	1.20×10^{-7}
25	0.45	3.86×10^{-13}	1.57×10^{-17}	1.17×10^{-16}	0.274	6.92	1.20×10^{-7}
30	0.45	3.16×10^{-13}	2.26×10^{-17}	9.22×10^{-17}	0.310	6.62	1.04×10^{-7}
20	0.55	3.95×10^{-13}	7.53×10^{-19}	1.23×10^{-16}	0.310	8.56	1.38×10^{-7}
25	0.55	5.20×10^{-13}	1.45×10^{-18}	1.45×10^{-16}	0.310	8.36	1.48×10^{-7}
30	0.55	3.56×10^{-13}	3.21×10^{-18}	1.15×10^{-16}	0.310	7.73	1.26×10^{-7}

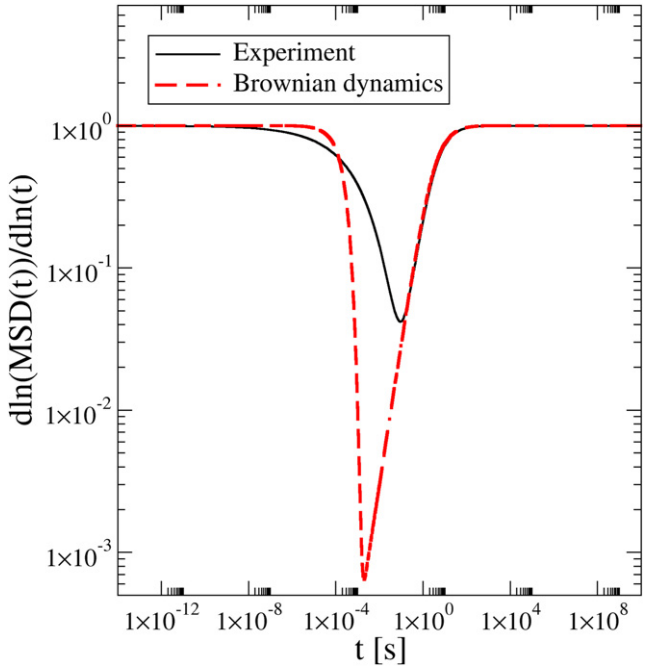

Figure 4. Logarithmic derivative of the mean square displacement MSD(t) displayed in figure 3.

for a particle in a parabolic potential, plus a smooth transition between short-times diffusion and a long-times diffusion regime, which is related to the escape of the particle from the potential. The Bellour equation has associated a logarithmic derivative given by:

$$\frac{\mathrm{d}\ \ln\ \mathrm{MSD}^{\mathrm{Bellour}}(t, D_0, D_{\mathrm{M}}, \alpha, \delta)}{\mathrm{d}\ \ln(t)} = t(\delta^2 + D_{\mathrm{M}}t)^{-1}\left(D_{\mathrm{M}} + D_0\left(1 + \frac{D_{\mathrm{M}}t}{\delta^2}\right)\left(\frac{D_0 t}{\delta^2}\right)^{\alpha-1} \times \exp\left\{-\left(\frac{D_0 t}{\delta^2}\right)^{\alpha}\right\}\left(1 - \exp\left\{-\left(\frac{D_0 t}{\delta^2}\right)^{\alpha}\right\}\right)^{-1}\right). \quad (5)$$

On the other side, the ratio of the long- and short-time diffusion coefficients can be calculated in terms of an effective one-dimensional periodic potential as:

$$\frac{D_{\mathrm{M}}}{D_0} = \frac{1}{\langle \exp\{U(x)/(k_{\mathrm{B}}T)\}\rangle \langle \exp\{-U(x)/(k_{\mathrm{B}}T)\}\rangle}, \quad (6)$$

where the brackets $\langle \ldots \rangle$ indicate the average over the unit cell [21]. At large values of U_0, equation (6) reduces to the following analytical formula:

$$\frac{D_{\mathrm{M}}}{D_0} = \frac{2\pi U_0}{k_{\mathrm{B}}T} \exp\left\{\frac{-2U_0}{k_{\mathrm{B}}T}\right\}. \quad (7)$$

Some error bounds of equation (7) as a function of U_0 have been discussed recently in reference [30].

The maximum height U_0 of the cosine potential given by equation (1) can be calculated from equation (6) if D_0^{Exp} and $D_{\mathrm{M}}^{\mathrm{Exp}}$ are known (e.g., from the Bellour fitting of equation (4)). At high values of U_0, the parameter α is approximately equal to 1 for the cosine potential given in equation (1) [30]. Our proposal is to use $D_0 = D_0^{\mathrm{Exp}}$ and U_0 in economic Brownian dynamics simulations in order to adjust the width L (of the effective periodic potential) until the MSD is approximately equal to the experimental one at the time t^*, at which a change of curvature is observed:

$$\mathrm{MSD}^{\mathrm{BD}}(t^*, L, D_0, U_0) \approx \mathrm{MSD}^{\mathrm{Exp}}(t^*, D_0^{\mathrm{Exp}}, D_{\mathrm{M}}^{\mathrm{Exp}}, \alpha^{\mathrm{Exp}}, \delta^{\mathrm{Exp}}). \quad (8)$$

Note that, in general, the value of t^* is different for the experimental and the BD MSD. However, this one-fitting parameter prescription is able to reproduce the experimental long-time MSD via economic BD simulations if the condition given by equation (8) is approximately fulfilled, as it is shown below.

3. Results and discussion

The activation energy in a WM solution is the height of the energy barrier that a tracer has to overcome in order to diffuse at long-times. In table 1, the experimental activation energies of a tracer in a WM solution at different temperatures and concentrations of surfactant and brine [34] are shown. By using the corresponding experimental diffusion coefficients and the equation (6), the amplitude U_0 of the one-dimensional periodic effective potential can be calculated. The

Table 3. Bellour parameters D_0^{Exp}, $D_{\text{M}}^{\text{Exp}}$, δ^{Exp}, and α^{Exp} associated to experimental MSD curves of a spherical tracer of 800 nm of diameter immersed in WM solutions with zwitterionic surfactant TDPS, anionic surfactant SDS and brine ($C_z = 46$ mM, $R = 0.55$, and $T = 25$ C) reported in reference [11] U_0 was obtained in this work from equation (6). By using D_0 and U_0 as fixed parameters in Brownian dynamics simulations, the width L of the periodic effective potential was adjusted until the simulation and experimental MSD were approximately the same at the critical time t^*, where a change of curvature in the MSD is observed.

[NaCl] (M)	D_0^{Exp} (m^2 s^{-1})	$D_{\text{M}}^{\text{Exp}}$ (m^2 s^{-1})	$2\delta^{2\text{Exp}}$ (m^2)	α^{Exp}	$U_0[k_{\text{B}}T]^{\text{This work}}$	L (m)$^{\text{This work}}$
0.2	4.41×10^{-13}	2.78×10^{-18}	1.28×10^{-16}	0.310	7.92	1.35×10^{-7}
0.225	5.20×10^{-13}	1.45×10^{-18}	1.45×10^{-16}	0.310	8.36	1.48×10^{-7}
0.3	4.83×10^{-13}	1.82×10^{-18}	1.24×10^{-16}	0.310	8.20	1.35×10^{-7}
0.4	3.81×10^{-13}	5.83×10^{-18}	1.37×10^{-16}	0.310	7.45	1.35×10^{-7}
0.5	3.68×10^{-13}	7.99×10^{-18}	8.14×10^{-17}	0.310	7.26	1.02×10^{-7}

Table 4. Bellour parameters D_0^{Exp}, $D_{\text{M}}^{\text{Exp}}$, δ^{Exp}, and α^{Exp} associated to experimental MSD curves of a spherical tracer of 800 nm of diameter immersed in WM solutions with zwitterionic surfactant TDPS, anionic surfactant SDS and brine ($C_z = 46$ mM, [NaCl] = 0.5 M, and $T = 25$ C) reported in reference [11] U_0 was obtained in this work from equation (6). By using $D_0 = D_0^{\text{Exp}}$ and U_0 as fixed parameters in Brownian dynamics simulations, the width L of the periodic effective potential was adjusted until the simulation and experimental MSD were approximately the same at the critical time t^*, where a change of curvature in the MSD is observed.

R	D_0^{Exp} (m^2 s^{-1})	$D_{\text{M}}^{\text{Exp}}$ (m^2 s^{-1})	$2\delta^{2\text{Exp}}$ (m^2)	α^{Exp}	$U_0[k_{\text{B}}T]^{\text{This work}}$	L (m)$^{\text{This work}}$
0.50	2.99×10^{-13}	9.19×10^{-18}	1.29×10^{-16}	0.310	7.07	1.28×10^{-7}
0.55	3.68×10^{-13}	7.99×10^{-18}	8.14×10^{-17}	0.310	7.26	1.02×10^{-7}
0.60	4.43×10^{-13}	3.16×10^{-17}	1.34×10^{-16}	0.310	6.62	1.25×10^{-7}

required energy to move a tracer to an adjacent cell in three dimensions can be approximated by $3U_0$ if the system is isotropic. This energy collates very well regarding the experimental activation energy under different conditions of temperature and concentrations of surfactant and brine, as it is shown in table 1.

Once U_0 has been determined, the width L of the effective periodic potential is fitted via economic Brownian dynamics simulations in which $D_0 = D_0^{\text{Exp}}$, in order to fulfill the equation (8) for a given Bellour parametrization of the experimental MSD (defined by the parameters D_0^{Exp}, $D_{\text{M}}^{\text{Exp}}$, δ^{Exp}, and α^{Exp}). In particular, a couple of typical Brownian dynamics and experimental time dependent mean square displacements $\text{MSD}^{\text{BD}}(t, L, D_0, U_0)$ and $\text{MSD}^{\text{Exp}}\left(t, D_0^{\text{Exp}}, D_{\text{M}}^{\text{Exp}}, \delta^{\text{Exp}}, \text{and } \alpha^{\text{Exp}}\right)$, respectively, are shown in figure 3. In the experimental system, the WM solution contains a zwitterionic surfactant (tetradecyl dimethylammonium propane sulfonate (TDPS)), an anionic surfactant (sodium dodecyl sulfate (SDS)), and brine at the following concentrations $C_z = 46$ mM, [NaCl] = 0.5 M, and $R = 0.45$, where C_z is the zwitterionic surfactant concentration and $R = [\text{SDS}]/[\text{TDPS}]$ is the surfactant ratio. The associated Bellour parameters in this instance are displayed in the second line of table 2 for $T = 25$ C. In this figure, it is observed that both MSD tend to the same limit at very short- and long-times. Both MSDs display approximately the same height of the plateau around the critical time t^*. The logarithmic derivatives associated to the MSDs shown in figure 3 are displayed in figure 4. Here, it is observed that both logarithmic derivatives tend to the same limit at very short- and long-times, displaying a minimum at t^* at intermediate times.

In tables 2–4, the one-dimensional effective periodic potential parameters U_0 and L associated to different experimental parametrizations of MSD are reported, for different temperatures and several concentrations of surfactant and brine. When these U_0 and L parameters are used in Brownian dynamics simulations with $D_0 = D_0^{\text{Exp}}$, the Bellour parametrization of the resulting MSD curves (via a nonlinear Marquardt–Levenberg least-squares minimization) produces the coefficients $D_0^{\text{BD}}, D_{\text{M}}^{\text{BD}}, \delta^{\text{BD}}, \alpha^{\text{BD}}$, coefficients. The first three parameters are consistent with the corresponding experimental coefficients $D_0^{\text{Exp}}, D_{\text{M}}^{\text{Exp}}, \delta^{\text{Exp}}$, as it is shown in figure 5. In addition, $\alpha^{\text{BD}} \approx 1$ as expected, considering the large values of U_0.

Two characteristic lengths of a WM solution are the mesh size ξ and the distance between entanglement points l_{e}. The elastic modulus G_0 of the WM solution is related to the network mesh size ξ through the formula [34] $G_0 \approx k_{\text{B}}T/\xi^3$. The entanglement length can be estimated as $l_{\text{e}} \approx \sqrt{3}\xi$ if the system is isotropic. In figure 6, L is compared to the experimental mesh size ξ and the entanglement length l_{e} for several temperatures and different concentrations of surfactant and brine. Here, it is observed that the width L of the periodic effective potential is an upper bound of the mesh size ξ, and it is of the same order of magnitude regarding the entanglement length l_{e} as a function of the temperature.

On the other hand, if L and D_{M} are known, it is possible to calculate the escape or hopping rate k_{escape} of the Brownian particle under the influence of the one-dimensional periodic potential defined by equation (1) via the equation [32]

$$D_{\text{M}} = D_{\text{eff}} = \frac{1}{2} k_{\text{escape}} L^2, \tag{9}$$

where $k_{\text{escape}} = 1/\tau_{\text{escape}}$ as shown in figure 2. In addition, let us define the MFPT τ_{MFPT} as the average time a Brownian particle needs to reach the separatrix manifold for the

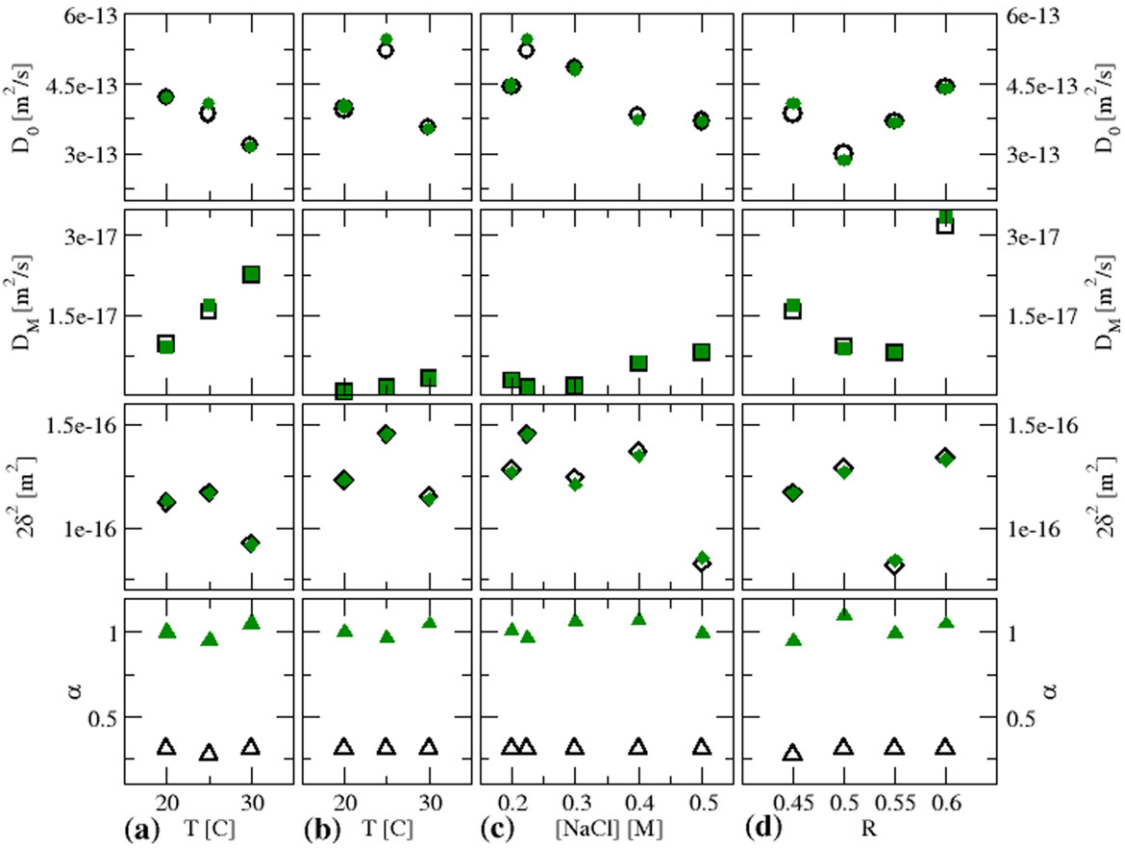

Figure 5. Bellour parameters D_0, D_M, δ, and α associated to experimental [11] and Brownian dynamics (this work) MSD curves of a spherical tracer of 800 nm of diameter immersed in WM solutions with zwitterionic surfactant TDPS, anionic surfactant SDS and brine. $C_z = 46$ mM in all panels. Column (a): the brine concentration is [NaCl] = 0.5 M and $R = 0.45$; column (b): the brine concentration is [NaCl] = 0.225 M and $R = 0.55$; column (c): the temperature is 25 C and $R = 0.55$; column (d): the temperature is 25 C and the brine concentration is [NaCl] = 0.5 M. Empty symbols correspond to experimental Bellour parameters D_0^{Exp}, D_M^{Exp}, δ^{Exp}, and α^{Exp} reported in reference [11] Solid symbols are the Bellour parameters D_0^{BD}, D_M^{BD}, δ^{BD}, and α^{BD} obtained via a non-linear Marquardt–Levenberg least-squares minimization of equation (4) from the Brownian dynamics MSD curves. Brownian dynamics used as input parameters $D_0 = D_0^{\mathrm{Exp}}$, U_0 and L, which are listed in tables 2–4.

first time when was located initially at a position x_0 inside the initial domain of attraction as shown in figure 2 for the cosine-like potential. Notice that at large height barriers, the MFPT $\tau_{\mathrm{MFPT}}(x_0)$ becomes essentially independent of the starting point, that is, $\tau_{\mathrm{MFPT}}(x_0)$ is approximately the same for all starting configurations away from the immediate neighborhood of the separatrix. If the probability of crossing the separatrix to the right or the left equals one half, the total escape time equals two times the MFPT, and the escape or hopping rate of the Brownian particle can be written as [30]:

$$k_{\mathrm{escape}} = \frac{1}{2\tau_{\mathrm{MFPT}}}. \tag{10}$$

Thus, equation (9) can be written in terms of the MFPT as:

$$D_M = \frac{1}{4\tau_{\mathrm{MFPT}}} L^2. \tag{11}$$

In terms of the effective periodic potential given by the equation (1), τ_{escape} can be written as [30]:

$$\tau_{\mathrm{escape}} = \tau_0 \langle \exp\{U(x)/(k_B T)\}\rangle \langle \exp\{-U(x)/(k_B T)\}\rangle, \tag{12}$$

where the brackets $\langle \ldots \rangle$ indicate the average over the unit cell, and

$$\tau_0 = \frac{L^2}{2D_0} \tag{13}$$

is the time that a particle needs to move a distance L in pure Brownian motion, that is, in the absence of any external potential, when the diffusion constant of the particle is D_0. At large values of U_0, equation (12) tends to the following analytical formula:

$$\tau_{\mathrm{escape}} \approx \frac{1}{2\pi}\tau_0 \frac{k_B T}{U_0} \exp\left\{\frac{2U_0}{k_B T}\right\}, \tag{14}$$

which corresponds to the Kramers approximation [30, 33]. Note that in the absence of an external potential (that is, in pure Brownian motion) τ_{escape} reduces to τ_0 according to equation (12) as expected, whereas τ_{escape} diverges to an infinite time according to the Kramers approximation given by equation (14) [30].

In figure 7, the experimental relaxation time of WM solutions, obtained from the crossover frequency between the elastic and viscous modulus in an oscillatory experiment and thus describing the onset of the transition from an purely elastic to a

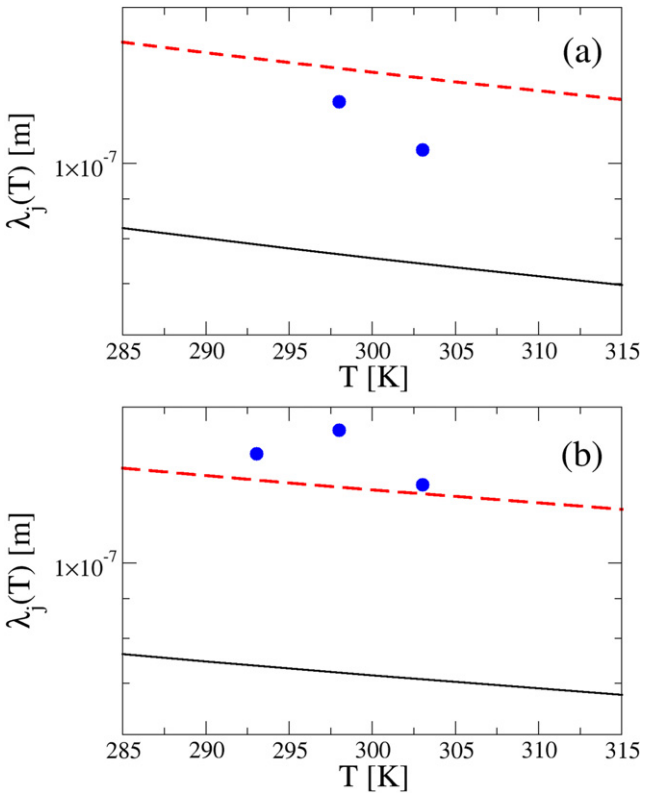

Figure 6. Experimental mesh size ξ (black continuous lines) and entanglement length l_e (red dashed lines) obtained from experimental WM solutions in reference [34], and numerical L values (solid circles, this work) associated to Brownian dynamics simulations, as a function of the temperature. In the experimental system, a spherical tracer of 800 nm of diameter is immersed in a WM solution with zwitterionic surfactant TDPS, anionic surfactant SDS and brine at different concentrations of surfactant and brine ($C_z = 46$ mM). (a) The brine concentration [NaCl] is 0.5 M and $R = 0.45$. (b) The brine concentration [NaCl] is 0.225 M and $R = 0.55$.

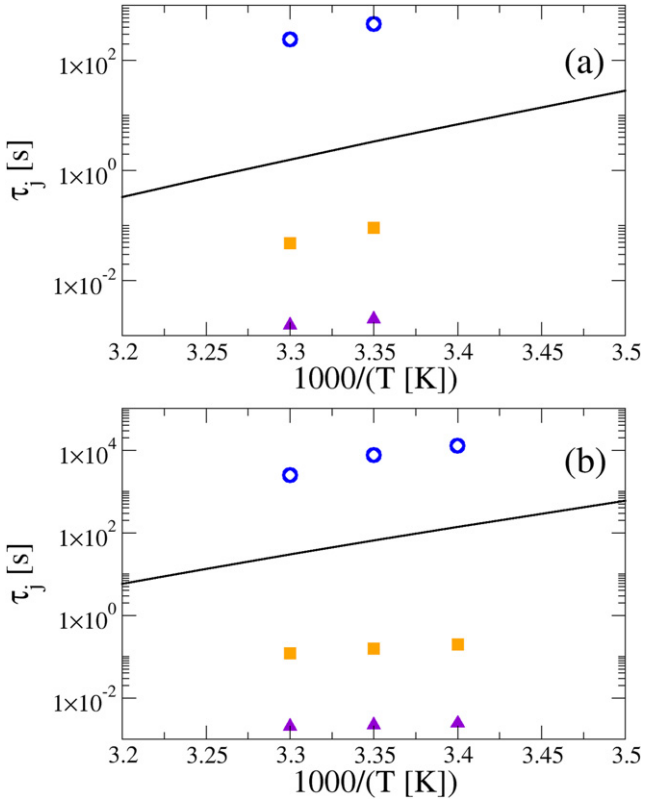

Figure 7. Experimental relaxation time τ_1 of WM solutions (black lines) corresponding to the data displayed in figure 6 as function of the temperature: in a) the brine concentration [NaCl] is 0.5 M and $R = 0.45$; and in (b) the brine concentration [NaCl] is 0.225 M and $R = 0.55$. The escape time τ_2 of a particle under the influence of an effective potential with length L (displayed as solid blue circles in figure 6 as a function of the temperature) is shown here as empty blue circles. Solid orange squares and purple triangles correspond to t^* calculated from the experimental, τ_3, and the effective potential, τ_4, Bellour parameters D_0, D_M, δ, and α (see, e.g., figures 4 and 5, and tables 2–4).

purely viscous response, corresponding to the data displayed in figure 6, as function of the temperature, is plotted. The escape time of a particle under the influence of an effective potential with the periodicity L displayed in figure 6 and the time t^* associated to the experimental and effective potential Bellour parameters (D_0, D_M, δ, and α) are also included in this figure. Here, it is seen that the t^* associated to the Bellour parameters (solid triangles) and the escape time of a Brownian particle under the influence of the effective cosine-like potential (empty circles), obtained via Brownian dynamics simulations, are lower and upper limits, respectively, for the experimental relaxation time of the WM solutions as a function of the temperature. On the other hand, in a recent study it has been shown that, for a Brownian particle under the influence of a periodic potential given by equation (1), t^* is located very close to the more likely MFPT at non-low height barriers U_0 [30]. Given that the values of t^* obtained from experiments and from the effective periodic potential approach are approximately of the same order of magnitude, we foresee that the experimental time t^* might be physically interpreted as an effective most likely hopping time of the tracer in the WM solution. As the relaxation time is related to the partial stress relaxation and the former quantity lies somewhere between the effective most likely hopping time of the tracer and the MFPT, the theoretical upper and lower bounds could be of help to extract an estimate of the experimental stress relaxation time. A more accurate estimation of this parameter would need a comprehensive study at different physical and chemical parameters and it is outside the scope of the present work.

4. Conclusions

In this work, we have proposed the use of Brownian dynamics of a single particle in the presence of a one-dimensional cosine-like potential to estimate the activation energy, the spatial confinement, and the mean first passage and escape times of a spherical tracer immersed in WM network, in which caging effects are observed experimentally. If the experimental 3D mean squared displacement of the tracer can be parametrized in terms of the short- and long-time diffusion coefficients, D_0 and D_M, respectively, as well as the parameters δ and α according to Bellour's prescription [31], U_0 can

be estimated from D_0 and D_M by following the Lifson and Jackson equation [21]. In order to estimate the effective confinement length L, we have proposed a one-fitting parameter method in which economic overdamped Brownian dynamics simulations are used. If D_0 and U_0 are fixed parameters in the Brownian dynamics simulations, the value of L is varied until the Brownian dynamics, and the experimental mean squared displacements match at the time t^*, where t^* denotes the inflexion point of the corresponding mean squared displacement. The proposed method has been used to characterize the long-time dynamics of WM solutions in the presence of a mixture of anionic and zwitterionic surfactants at several temperatures and at different concentrations of surfactant and brine. In particular, the amplitude U_0 has displayed a good agreement regarding the corresponding experimental activation energy at different temperatures. The periodicity L has shown to be an upper bound of ξ and to be of the same order of magnitude regarding l_e, where ξ and l_e are the mesh size and the distance between two entanglement points, respectively, obtained from rheology and microrheology experiments. The MFPT and the escape or hopping time of the tracer can be obtained straightforwardly from D_M and L. The escape time of the tracer and t^* are upper and lower limits, respectively, of the experimental relaxation time. In addition, the experimental time t^* might be interpreted as an effective most likely hopping time of the tracer in the polymeric solution. In summary, the proposed method to characterize the experimental long-time behaviour of a WM solution is simple and fast, and can be used to extract useful information of the complex network. We foresee that a similar methodology should be applicable to model the long-time behaviour of tracers in a wide variety of scenarios, where an energy barrier close to the thermal energy is present and a periodic structure is found at the macro scale, such as other polymer networks or colloidal systems. The colloidal glass transition is an example of this application and further studies could enlighten the possible impact on the understanding of such processes using this simple method.

Acknowledgments

ES-G acknowledges CONACYT Mexico through Grant A1-S-9098 and Grant Ciencia de Frontera 102986. GIG-G acknowledges the SEP-CONACYT CB-2016 Grant 286105, the 2019 Marcos Moshinsky Fellowship, and the National Supercomputing Center-IPICYT for the computational resources supported in this research through the Grant TKII-IVGU001; as well as the computing time granted by LANCAD and CONACYT on the supercomputer Yoltla/Miztli/Xiuhcoatl at LSVP UAM-Iztapalapa/DGTIC UNAM/CGSTIC CINVESTAV with the project 58-2021. GIG-G also express his gratitude for the assistance from the computer technicians at the IF-UASLP.

Data availability statement

The data that support the findings of this study are available upon reasonable request from the authors.

ORCID iDs

Guillermo Iván Guerrero-García https://orcid.org/0000-0002-3174-2643
Erick Sarmiento Gómez https://orcid.org/0000-0001-6130-4161

References

[1] Israelachvili J N 2008 *Intermolecular and Surface Forces* 3rd edn (New York: Academic)
[2] Israelachvili J N, Mitchell D J and Ninham B W 1976 *J. Chem. Soc. Faraday Trans. II* **72** 1525–68
[3] Marques E F and Silva B F B 2013 *Encyclopedia of Colloid and Interface Science* (Berlin: Springer)
[4] Dreiss C A 2007 *Soft Matter* **3** 956–70
[5] Graessley W and McLeish T 2004 The Doi–Edwards theory *Stealing the Gold: A Celebration of the Pioneering Physics of Sam Edwards* (Oxford: Oxford University Press)
[6] Cates M E 2007 *Macromolecules* **20** 2289–96
[7] Cates M E and Candau S J 1990 *J. Phys.: Condens. Matter* **2** 6869–92
[8] Dan N and Safran S A 2006 *Adv. Colloid Interface Sci.* **123–126** 323–31
[9] Oelschlaeger C, Suwita P and Willenbacher N 2010 *Langmuir* **26** 7045–53
[10] Willenbacher N, Oelschlaeger C, Schopferer M, Fischer P, Cardinaux F and Scheffold F 2007 *Phys. Rev. Lett.* **99** 068302
[11] Sarmiento-Gomez E, Lopez-Diaz D and Castillo R 2010 *J. Phys. Chem.* B **114** 12193–202
[12] Papagiannopoulos A, Vlassi E, Pispas S, Tsitsilianis C and Radulescu A 2021 *Macromol* **1** 37–48
[13] Pescosolido L *et al* 2012 *Soft Matter* **8** 7708–15
[14] Allen M P and Tildesley D J 1987 *Computer Simulation of Liquids* (New York: Oxford University Press)
[15] Barhoum S, Palit S and Yethiraj A 2016 *Prog. Nucl. Magn. Reson. Spectrosc.* **94–95** 1–10
[16] Holder S W, Grant S C and Mohammadigoushki H 2021 *Langmuir* **37** 3585–96
[17] Lopez-Gonzalez M R, Holmes W M and Callaghan P T 2006 *Soft Matter* **2** 855–69
[18] Macosko C W 2008 *Rheology Principles, Measurements, and Applications* (New York: Weinheim Cambridge VCH)
[19] Furst E M and Todd M S 2017 *Microrheology* (Oxford: Oxford University Press)
[20] Mason T G and Weitz D A 1995 *Phys. Rev. Lett.* **74** 1250–3
[21] Lifson S and Jackson J L 1962 *J. Chem. Phys.* **36** 2410–4
[22] Gunther L, Revzen M and Ron A 1979 *Physica* A **95** 367–9
[23] Weaver D L 1997 *Physica* A **98** 359–62
[24] Ermak D L 1975 *J. Chem. Phys.* **62** 4189–96
[25] Wei Q-H, Bechinger C, Rudhardt D and Leiderer P 1998 *Phys. Rev. Lett.* **81** 2606–9
[26] Herrera-Velarde S and Castañeda-Priego R 2007 *J. Phys.: Condens. Matter* **19** 226215

[27] Sarmiento-Gómez E, Rivera-Morán J A and Arauz-Lara J L 2019 *Soft Matter* **15** 3573–9
[28] Dalle-Ferrier C, Krüger M, Hanes R D L, Walta S, Jenkins M C and Egelhaaf S U 2011 *Soft Matter* **7** 2064–75
[29] Euán-Díaz E C, Misko V R, Peeters F M, Herrera-Velarde S and Castañeda-Priego R 2011 *Phys. Rev.* E **86** 031123
[30] Pérez-Guerrero D, Arauz-Lara J L, Sarmiento-Gómez E and Guerrero-García G I 2021 *Front. Phys.* **9** 635269
[31] Bellour M, Skouri M, Munch J-P and Hébraud P 2020 *Eur. Phys. J.* E **8** 431–6
[32] Ferrando R, Spadacini R and Tommei G E 1993 *Phys. Rev.* E **48** 2437–51
[33] Hänggi P, Talkner P and Borkovec M 1990 *Rev. Mod. Phys.* **62** 251–341
[34] Lopez-Diaz D and Castillo R 2010 *J. Phys. Chem.* B **114** 8917–25